Proceedings of the 16th International IEEE Annual Conference on Intelligent Transportation Systems (ITSC 2013), The Hague, The Netherlands, October 6-9, 2013

Graceful Degradation of CACC Performance Subject to Unreliable Wireless Communication

Jeroen Ploeg, Elham Semsar-Kazerooni, Guido Lijster,
Nathan van de Wouw, and Henk Nijmeijer, *Fellow, IEEE*

***Abstract*— Cooperative Adaptive Cruise Control (CACC) employs wireless intervehicle communication, in addition to onboard sensors, to obtain string-stable vehicle-following behavior at small intervehicle distances. As a consequence, however, CACC is vulnerable to communication impairments such as packet loss, in which case it would effectively degrade to conventional Adaptive Cruise Control (ACC), thereby increasing the minimal intervehicle distance needed for string-stable behavior. Therefore, a control strategy for graceful degradation of one-vehicle look-ahead CACC is proposed to partially maintain the string stability properties of CACC. This strategy is based on estimating the preceding vehicle's information, here acceleration, using the onboard sensors. Whenever needed, this estimated acceleration can be used as an alternative to the desired acceleration transmitted through wireless communication for this type of CACC. It is shown through simulations and experiments that the proposed strategy results in a noticeable improvement of string stability characteristics, when compared to the situation in which ACC is used as a fallback scenario.**

I. Introduction

Cooperative Adaptive Cruise Control (CACC) is essentially a vehicle-following control system that automatically accelerates and decelerates so as to keep a desired distance to the preceding vehicle [1]. To this end, onboard sensors are employed, such as radar, that measure the intervehicle distance and relative velocity. In addition, extra information of the preceding vehicle(s), e.g., the desired acceleration, is cast through a wireless communication link. As a consequence, the performance in terms of minimizing the intervehicle distance while guaranteeing string stability, i.e., shock wave attenuation in upstream direction, is significantly enhanced when compared to conventional Adaptive Cruise Control (ACC), which is operated without wireless communication link. As a result, traffic throughput is increased, while maintaining a sufficient level of safety [2], although string-stable behavior *per se* does not guarantee the avoidance of collisions. In addition, significant fuel savings are possible, especially for trucks [3].

Inherent to the CACC concept is its vulnerability to unreliable wireless communication due to high latency or packet loss. In [4], for instance, it was found that the ratio of correctly received packets drops below 10 % on a motorway junction with high traffic density, assuming all vehicles are communicating. The relation between latency or packet loss and string stability of CACC already attracted interest, see, e.g., [5]. In addition to the existing literature on this topic, this paper focusses on losing the wireless communication link for an extended period of time. In this case, while not taking any compensating actions, CACC inherently degrades to ACC, which requires a significantly larger time headway for string-stable behavior. As an example, [6] shows that the minimum string-stable time headway increases from 0.25 s to more than 3 s. It is, therefore, important to have an alternative control technique that exhibits string-stable behavior for a less dramatic increase in time headway, which comes into action when a failure in the wireless communication is detected. To this end, this paper presents a fallback strategy to gracefully degrade functionality of a one-vehicle look-ahead CACC, based on estimating the preceding vehicle's acceleration using the available data from an onboard sensor.

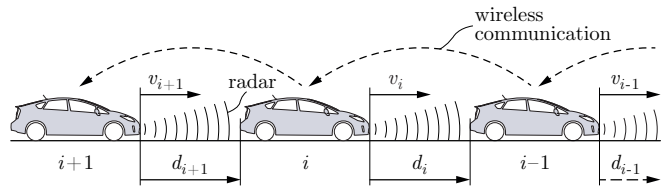

Fig. 1. A homogeneous platoon of vehicles equipped with CACC.

This paper is organized as follows. Section II first provides an overview of the adopted CACC and the notion of string stability used in the present work. Next, Section III introduces the graceful degradation strategy, upon which Section IV analyses the string stability properties of the controlled system, in comparison to those of ACC and CACC. Section V then presents experimental results obtained with two CACC-equipped passenger vehicles. Finally, Section VI summarizes the main conclusions.

II. Control of vehicle platoons

Consider a platoon of m vehicles as shown in Fig. 1 where the vehicles are enumerated with index $i = 1, \ldots, m$, with $i = 1$ indicating the lead vehicle. From the perspective of road usage efficiency, it is desired that a short intervehicle distance d_i is maintained within this platoon. ACC addresses this need with the help of vehicle measurement devices, e.g., radar or lidar, which measure the relative velocity and the

This work is funded by the Dutch Ministry of Economic Affairs through the High Tech Automotive Systems (HTAS) project Connected Cruise Control, and by the TNO Program on Adaptive Multi-Sensor Networks.

J. Ploeg and E. Semsar-Kazerooni are with TNO Automotive, P.O. Box 756, 5700 AT Helmond, The Netherlands, jeroen.ploeg@tno.nl, elham.semsarkazerooni@tno.nl

G. Lijster is with TMC Mechatronics, Eindhoven, The Netherlands, guido.lijster@tmc.nl

N. van de Wouw and H. Nijmeijer are with the Eindhoven University of Technology, Mechanical Engineering Department, Eindhoven, The Netherlands, n.v.d.wouw@tue.nl, h.nijmeijer@tue.nl

978-1-4799-2914-613/$31.00 ©2013 IEEE

distance with respect to the preceding vehicle. A weakness of ACC, however, is its inability to attenuate traffic shock waves, e.g., caused by sudden braking or velocity decrease by a vehicle within the platoon, in an upstream direction, unless a large intervehicle distance is chosen [7]. This property of shockwave attenuation is referred to as string stability.

A. String stability of a vehicle platoon

In the literature, three main directions towards defining the notion of string stability can be distinguished: 1) a formal Lyapunov-stability approach [8], 2) a stability approach for spatially-invariant linear systems [9], and 3) a performance-oriented frequency-domain approach [1]. Due to its capability of offering controller synthesis tools, the last approach is more often used in the literature. In [6], an overview of the most relevant literature in this respect is given, based on which a general string stability definition is proposed and, based on this generic defintion, string stability conditions for linear unidirectionally-coupled homogeneous systems are given that correspond to the conditions used in the performance-oriented approach. This subsection briefly summarizes these conditions.

Let the homogeneous vehicle platoon, in which all follower vehicles are controlled by a one-vehicle look-ahead CACC, be formulated by the following state-space model (omitting the time argument t for readability):

$$\begin{pmatrix} \dot{x}_1 \\ \dot{x}_2 \\ \vdots \\ \dot{x}_m \end{pmatrix} = \begin{pmatrix} A_0 & & & \mathrm{O} \\ \tilde{A}_1 & \tilde{A}_0 & & \\ & \ddots & \ddots & \\ \mathrm{O} & & \tilde{A}_1 & \tilde{A}_0 \end{pmatrix} \begin{pmatrix} x_1 \\ x_2 \\ \vdots \\ x_m \end{pmatrix} + \begin{pmatrix} B_0 \\ 0 \\ \vdots \\ 0 \end{pmatrix} u_1 \quad (1)$$

or, in short,

$$\dot{x} = Ax + Bu_1 \quad (2)$$

with $x^{\mathrm{T}} = \begin{pmatrix} x_0^{\mathrm{T}} & x_1^{\mathrm{T}} & \dots & x_m^{\mathrm{T}} \end{pmatrix}$, and the matrices A and B defined accordingly. x_i, $i \in S_m$, is the state vector of vehicle i (typically containing distance or distance error, position, velocity, acceleration, and possibly additional variables), with $S_m = \{i \in \mathbb{N} \mid 1 \leq i \leq m\}$ denoting the set of all vehicles in a platoon of length $m \in \mathbb{N}$. u_1 is the external input, which, in this case, is the input of the uncontrolled lead vehicle. A_0 and B_0 are the system matrix and input matrix, respectively, of the lead vehicle, whereas $\tilde{A}_0$ and $\tilde{A}_1$ are the system and "input" matrix, respectively, of the controlled follower vehicles. In addition, consider linear output functions according to

$$y_i = C_i x, \quad i \in S_m \quad (3)$$

where y_i is the output of vehicle i, and C_i the corresponding output matrix. The model (2), (3), which will be further detailed in Section II-B, is considered $\mathcal{L}_p$ *string stable* if all outputs y_i are bounded (in the $\mathcal{L}_p$ sense) for a bounded input u_1 and bounded initial condition perturbations $x(0)$ with $m \to \infty$, i.e., infinite string length. Hence, $y_i(t)$ must be bounded for all $i \in \mathbb{N}$ and for all $t \geq 0$. If, in addition,

$$\|y_i(t) - C_i\bar{x}\|_{\mathcal{L}_p} \leq \|y_{i-1}(t) - C_{i-1}\bar{x}\|_{\mathcal{L}_p}, \ \forall\, i \in \mathbb{N}\backslash\{1\} \quad (4)$$

where $\bar{x}$ denotes the equilibrium state of (2) with $u_1 \equiv 0$ and $\|\cdot\|_{\mathcal{L}_p}$ denotes the signal p-norm, the interconnected system is said to be *strictly $\mathcal{L}_p$ string stable*.

Remark 1: For linear homogeneous cascaded systems with a unidirectional coupling, and with a scalar input u_1 and scalar outputs y_i, the notions of $\mathcal{L}_p$ string stability and strict $\mathcal{L}_p$ string stability are equivalent [6]. $\Diamond$

Reformulating (2), (3) in the Laplace domain, while exclusively focussing on input–output behavior, yields

$$y_i(s) = P_i(s)u_1(s), \quad i \in S_m \quad (5)$$

where $y_i(s)$ and $u_1(s)$, $s \in \mathbb{C}$, denote the Laplace transforms of $y_i(t)$ and $u_1(t)$, respectively, and $P_i(s) = C_i(sI - A)^{-1}B$. Assuming that the system (5) is square and functionally controllable (i.e., $P_i^{-1}(s)$ exists for all $i \in S_m$), the *string stability complementary sensitivity* (SSCS) is defined as

$$\Gamma_i(s) := P_i(s)P_{i-1}^{-1}(s) \quad (6)$$

such that $y_i(s) = \Gamma_i(s)y_{i-1}(s)$. Adopting the $\mathcal{L}_2$ signal norm (i.e., $p = 2$), the following condition for strict $\mathcal{L}_2$ string stability then holds [6].

Condition 1 (Strict $\mathcal{L}_2$ String Stability): The system (2), (3), with Laplace-domain representation (5), is strictly $\mathcal{L}_2$ string stable if and only if

$$\|P_1(s)\|_{\mathcal{H}_\infty} < \infty \quad (7a)$$

$$\|\Gamma_i(s)\|_{\mathcal{H}_\infty} \leq 1, \quad \forall\, i \in \mathbb{N}\backslash\{1\} \quad (7b)$$

where $\Gamma_i(s)$ is the SSCS according to (6) and $\|\cdot\|_{\mathcal{H}_\infty}$ denotes the $\mathcal{H}_\infty$ system norm.

As mentioned before, ACC is not efficient in maintaining string stability in a platoon of vehicles. As a result, in the early 90's the concept of platooning with the help of wireless information has been introduced [1]. Nowadays, the resulting control strategies are referred to as Cooperative Adaptive Cruise Control (CACC). The next subsection presents an overview of the CACC strategy employed in this paper.

B. Cooperative Adaptive Cruise Control

The objective of CACC is to guarantee that, within a string of vehicles, the intervehicle distances d_i, $i \in S_m\backslash\{1\}$, are regulated to a safe but small value. In addition, this string should be able to attenuate the shock waves that arise as a result of a sudden change in the state of a vehicle in the platoon due to, e.g., braking. In the following, a control design strategy is briefly explained which guarantees that the above objectives are satisfied. Although the results obtained in the present paper are rather generic and independent of the selected CACC strategy, a specific CACC structure is chosen to be able to proceed with the details of the proposed method, being the one-vehicle look-ahead CACC as developed and experimentally validated in [7].

Consider the following model of a vehicle within a platoon of m vehicles as shown in Fig. 1:

$$\begin{pmatrix} \dot{d}_i \\ \dot{v}_i \\ \dot{a}_i \end{pmatrix} = \begin{pmatrix} v_{i-1} - v_i \\ a_i \\ -\frac{1}{\tau}a_i + \frac{1}{\tau}u_i \end{pmatrix}, \quad i \in S_m\backslash\{1\} \quad (8)$$

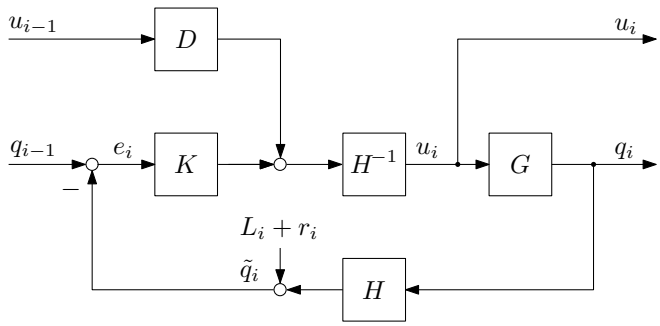

Fig. 2. Block scheme of the CACC system.

with $d_i = q_{i-1} - q_i - L_i$ being the distance between vehicle i and $i-1$, where q_i and q_{i-1} are the rear bumper position of vehicle i and $i-1$, respectively, and L_i is the length of vehicle i; v_i is the velocity and a_i is the acceleration of vehicle i. Moreover, u_i is the vehicle input, to be interpreted as desired acceleration, and τ is the time constant representing the driveline dynamics. Also, the following policy for the intervehicle spacing is adopted:

$$d_{r,i}(t) = r_i + hv_i(t), \quad i \in S_m \backslash \{1\} \tag{9}$$

where $d_{r,i}$ is the desired distance between vehicle i and $i-1$, h is the time headway, and r_i is the standstill distance. The main objective is to regulate the distances d_i to $d_{r,i}(t)$, i.e.,

$$e_i(t) = d_i(t) - d_{r,i}(t) \to 0 \text{ as } t \to \infty \tag{10}$$

while allowing for the fact that (10) may only be satisfied if the lead vehicle drives with a constant velocity, i.e., $a_1 = 0$.

In [7], it is shown that the following dynamic controller achieves this vehicle-following objective:

$$\dot{u}_i = -\frac{1}{h}u_i + \frac{1}{h}(k_p e_i + k_d \dot{e}_i + k_{dd}\ddot{e}_i) + \frac{1}{h}u_{i-1} \tag{11}$$

where k_p, k_d, and k_{dd} are the controller coefficients. Furthermore, it is shown that for a bounded u_{i-1} and subject to the following constraints on the controller gains: $k_p, k_d > 0$, $k_{dd} + 1 > 0$, $(1 + k_{dd})k_d - k_p\tau > 0$, the intervehicle distance d_i is regulated to $d_{r,i}$ as defined by the spacing policy (9), thus satisfying (10). The block diagram of the closed-loop system for vehicle i, subject to the controller (11), is shown in Fig. 2, with

$$\begin{aligned} G(s) &= \frac{q_i(s)}{u_i(s)} = \frac{1}{s^2(\tau s + 1)} \\ H(s) &= hs + 1 \\ K(s) &= k_p + k_d s + k_{dd}s^2 \\ D(s) &= e^{-\theta s}. \end{aligned} \tag{12}$$

Here, $q_i(s)$ and $u_i(s)$ are the Laplace transforms of the vehicle position $q_i(t)$ and the desired acceleration $u_i(t)$, respectively; the vehicle transfer function $G(s)$ follows from $\dddot{q}_i = -\frac{1}{\tau}\ddot{q}_i + \frac{1}{\tau}u_i$, see (8), whereas the spacing policy transfer function $H(s)$ is related to (9) and the controller $K(s)$ represents the error feedback in (11). Also, θ is the time delay induced by the wireless communication network. The above setup is used for the purpose of controller design. However, in experimental identification of the vehicle dynamics [7], it was noticed that another delay needs to be included in the transfer function $G(s)$ in order to model the delay in the vehicle's actuation mechanism. Hence, in the remainder of this paper it is assumed that

$$G(s) = \frac{1}{s^2(\tau s + 1)}e^{-\phi s} \tag{13}$$

where ϕ is the vehicle time delay.

Now let the vehicle acceleration be taken as a basis for string stability, i.e., $y_i(t) = a_i(t)\ \forall i \in S_m$, since it is physically relevant on the one hand, and satisfies the norm requirement on $P_1(s)$ in Condition 1 on the other hand. The latter can be easily understood, because, with this choice of outputs, $P_1(s) = \frac{1}{\tau s+1}e^{-\phi s}$, hence $\|P_1(j\omega)\|_{\mathcal{H}_\infty} = 1$. The corresponding SSCS is then given by

$$\Gamma_{CACC}(s) = \frac{a_i(s)}{a_{i-1}(s)} = \frac{1}{H(s)}\frac{G(s)K(s) + D(s)}{1 + G(s)K(s)} \tag{14}$$

where $a_i(s)$ and $a_{i-1}(s)$ are the Laplace transforms of $a_i(t)$ and $a_{i-1}(t)$, respectively. Note that, without loss of generality, $r_i = L_i = 0\ \forall i \in S_m \backslash \{1\}$ is assumed. Furthermore, it is noted that the SSCS (14) would be the same in case the velocity v_i is chosen as output, since $\frac{a_i(s)}{a_{i-1}(s)} = \frac{sv_i(s)}{sv_{i-1}(s)} = \frac{v_i(s)}{v_{i-1}(s)}$, but that the first requirement in Condition 1 would not be satisfied in that case. In addition, it is worth mentioning that the SSCS is independent of the vehicle index i, which is a direct consequence of the homogeneity assumption. Finally, it appears that for an ACC system, i.e., where no feedforward path exists, the SSCS $\Gamma_{ACC}(s)$ can be obtained from (14) with $D(s) = 0$:

$$\Gamma_{ACC}(s) = \frac{1}{H(s)}\frac{G(s)K(s)}{1 + G(s)K(s)}. \tag{15}$$

III. Graceful degradation

The main difference of the CACC proposed in the previous section with its ACC counterpart is in the feedforward path, see Fig. 2, which includes the effect of the preceding vehicle's desired acceleration u_{i-1} into the control loop. However, this feedforward path depends on the quality of the wireless intervehicle communication, in terms of latency and packet loss. Consequently, if the wireless communication fails, CACC would automatically degrade to ACC, leading to a significant increase in minimal time headway to maintain string-stable behavior. It is, therefore, desirable to implement an alternative fallback scenario, i.e., a graceful degradation technique, with less dramatic consequences. To this end, it is proposed to estimate the actual acceleration of the preceding vehicle, which can then be used as a replacement of the desired acceleration in case no communication updates are received. To arrive at an accurate acceleration estimation, Section III-A first describes a dynamic model for the target vehicle as a basis for state estimation, after which Section III-B incorporates the acceleration estimation algorithm into the CACC framework.

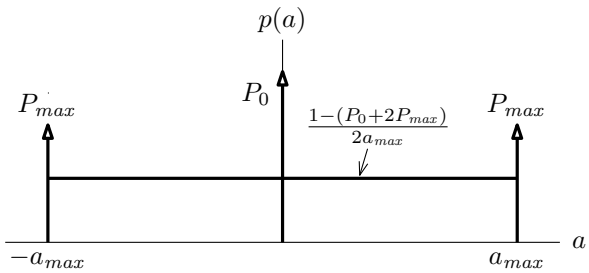

Fig. 3. Probability density function $p(a)$ of the object acceleration a.

A. Object tracking

Since there might be several object vehicles close to the follower vehicle, a multi-object tracking algorithm needs to be applied, which is able to distinguish and track the desirable object in a multi-object environment. This involves, firstly, associating the correct measurement data with the various tracked objects and, secondly, estimating the objects' states. In the scope of this paper, the focus is on the estimation technique. Moreover, regardless of the specific estimation technique, a dynamical object model has to be adopted for the estimation algorithm, that represents the target's pattern of motion as good as possible. In the following, a concise description is given of the dynamic object model as well as the estimation technique applied here.

1) Dynamic object model: In order to describe an object's longitudinal motion, the Singer acceleration model [10] is adopted here, since this model appears to provide a good approximation of the longitudinal vehicle dynamics [11]. This model takes into account the correlation in time of the acceleration, namely if a target is accelerating at time instant t, it is likely to be accelerating at time instant $t+\tau$ for a sufficiently small τ. This time correlation results in the following state equation of a linear time-invariant system describing the vehicle acceleration:

$$\dot{a}(t) = -\alpha a(t) + u(t) \tag{16}$$

with a being the acceleration of the object vehicle, $\alpha = 1/\tau_m$, where τ_m is the so-called maneuver time constant, and u being the model input. Since u is unknown, the *equivalent-noise approach* [12] is chosen, by assuming that this input is a zero-mean uncorrelated random process (white noise). To arrive at the statistical characteristics of this white noise, the object vehicle is assumed to exhibit maximum acceleration a_{max} or deceleration $-a_{max}$ with a probability P_{max} and to have a probability P_0 of zero acceleration, whereas other acceleration values are uniformly distributed. This results in the probability density function $p(a)$ for the object acceleration a as shown in Fig. 3, which appeared to provide a satisfactory representation of the object's instantaneous maneuver characteristics [10]. Consequently, the variance σ_a^2 of the object acceleration equals

$$\sigma_a^2 = \frac{a_{max}^2}{3}(1 + 4P_{max} - P_0). \tag{17}$$

It can then be shown [10] that, in order to satisfy $p(a)$, the covariance $C_{uu}(\tau)$ of the white-noise input u in (16) must be equal to

$$C_{uu}(\tau) = 2\alpha\sigma_a^2\delta(\tau). \tag{18}$$

As a result, the random variable a, satisfying a probability density function $p(a)$ with variance σ_a^2 as in (17), while being correlated in time through the maneuver time constant τ_m, is described as a random process $a(t)$, being the output of a first-order system (16) with a white-noise input $u(t)$ satisfying (18).

Using the acceleration model (16), the corresponding equation of motion can be formulated in the state space as

$$\dot{x}(t) = Ax(t) + Bu(t) \tag{19a}$$

$$y(t) = Cx(t) \tag{19b}$$

where $x^{\mathrm{T}} = \begin{pmatrix} q & v & a \end{pmatrix}$, with q and v being the object vehicle's position and velocity, respectively. The vector $y^{\mathrm{T}} = \begin{pmatrix} q & v \end{pmatrix}$ is the output of the model and the matrices A, B, and C are defined as follows:

$$A = \begin{pmatrix} 0 & 1 & 0 \\ 0 & 0 & 1 \\ 0 & 0 & -\alpha \end{pmatrix},\ B = \begin{pmatrix} 0 \\ 0 \\ 1 \end{pmatrix},\ C = \begin{pmatrix} 1 & 0 & 0 \\ 0 & 1 & 0 \end{pmatrix}. \tag{20}$$

Note that the state equation (19a) closely resembles the vehicle dynamics model (8) when replacing α by τ^{-1}. Moreover, $Bu(t)$ is a white-noise signal, which can thus be regarded as the process noise in the estimator design described in the next subsection.

2) Estimation technique: The approach that is adopted for estimation of the object vehicle acceleration, is the stand-alone Kalman filter, where estimations of the internal state of a linear dynamical system are based on the observations of the sensors only [13]. Obviously, for real-time implementation in the vehicle control computer, a discrete-time Kalman filter is required. However, in view of the upcoming string stability analysis, the continuous-time equivalent of the Kalman filter will be employed here. This Kalman filter is based on the state-space model

$$\begin{aligned} \dot{x}(t) &= Ax(t) + w(t) \\ y(t) &= Cx(t) + v(t) \end{aligned} \tag{21}$$

which corresponds to (19) and (20), with an additional measurement noise vector $v(t)$ and the process noise equal to $w(t) = Bu(t)$, according to the equivalent-noise approach. $v(t)$ is a Gaussian white-noise signal, the covariance matrix $R = E\{v(t)v^{\mathrm{T}}(t)\}$ of which is chosen based on the noise parameters of the onboard sensor used in the implementation of the observer, which, in this case, is a radar (refer to Section V). Furthermore, using (18), the continuous-time process noise covariance matrix $Q = E\{w(t)w^{\mathrm{T}}(t)\}$ equals

$$Q = BB^{\mathrm{T}}E\{u(t)u^{\mathrm{T}}(t)\} = \begin{pmatrix} 0 & 0 & 0 \\ 0 & 0 & 0 \\ 0 & 0 & 2\alpha\sigma_a^2 \end{pmatrix}. \tag{22}$$

With the given Q and R matrices, the following continuous-time observer is obtained:

$$\dot{\hat{x}}(t) = A\hat{x}(t) + L\big(y(t) - C\hat{x}(t)\big) \tag{23}$$

with A and C according to (20). $\hat{x}$ is estimate of the object vehicle state $x^{\mathrm{T}} = \begin{pmatrix} q & v & a \end{pmatrix}$ and L is the continuous-time Kalman filter gain matrix.

B. CACC fallback scenario

The "degraded" CACC (dCACC) employs the estimated acceleration rather than the desired acceleration of the preceding vehicle[1]. However, the inputs of the acceleration estimator, being the absolute object position and velocity, cannot be measured. Instead, the onboard sensor provides distance and relative velocity. The estimation algorithm thus needs to be adapted, as explained in this subsection.

As a first step, the continuous-time estimator (23) is described in the Laplace domain by a transfer function $T(s)$, which takes the actual position q_{i-1} and velocity v_{i-1} of the preceding vehicle, contained in the measurement vector $y(t)$ in (23), as the input, and has the estimate $\hat{a}_{i-1}$ of this vehicle's acceleration, being the third element of the estimated state, as the output. This yields

$$\hat{a}_{i-1}(s) = T(s) \begin{pmatrix} q_{i-1}(s) \\ v_{i-1}(s) \end{pmatrix} \tag{24}$$

where $\hat{a}_{i-1}(s)$ denotes the Laplace transform of $\hat{a}_{i-1}(t)$, and $q_{i-1}(s)$ and $v_{i-1}(s)$ are the Laplace transforms of $q_{i-1}(t)$ and $v_{i-1}(t)$, respectively. Moreover, the 1×2 observer transfer function $T(s)$ equals

$$T(s) = \hat{C}(sI - \hat{A})^{-1}\hat{B} := \begin{pmatrix} T_{qa}(s) & T_{va}(s) \end{pmatrix} \tag{25}$$

with $\hat{A} = A - LC$, $\hat{B} = L$, and $\hat{C} = \begin{pmatrix} 0 & 0 & 1 \end{pmatrix}$. Note that $T(s)$ does not depend on the vehicle index i due to the homogeneity assumption.

The second step involves a transformation to relative coordinates, using the fact that (with $L_i = 0$)

$$\begin{aligned} q_{i-1}(s) &= d_i(s) + q_i(s) \\ v_{i-1}(s) &= \Delta v_i(s) + v_i(s), \end{aligned} \tag{26}$$

where $\Delta v_i(s)$ denotes the Laplace transform of the relative velocity $\Delta v_i(t) = \dot{d}_i(t)$. Substituting (26) into (24) yields

$$\begin{aligned} \hat{a}_{i-1}(s) &= T(s) \begin{pmatrix} d_i(s) \\ \Delta v_i(s) \end{pmatrix} + T(s) \begin{pmatrix} q_i(s) \\ v_i(s) \end{pmatrix} \\ &:= \widehat{\Delta a}_i(s) + \hat{a}_i(s). \end{aligned} \tag{27}$$

As a result, the acceleration estimator is split into a relative-coordinate estimator $\widehat{\Delta a}_i(s) := T(s)\big(d_i(s)\ \Delta v_i(s)\big)^{\mathrm{T}}$, where $\widehat{\Delta a}_i(s)$ can be regarded as the Laplace transform of the estimated relative acceleration $\widehat{\Delta a}_i(t)$, and an absolute-coordinate estimator $\hat{a}_i(s) = T(s)\big(q_i(s)\ v_i(s)\big)^{\mathrm{T}}$, where $\hat{a}_i(s)$ is the Laplace transform of the estimated local acceleration $\hat{a}_i(t)$.

Finally, $\hat{a}_i(s)$ in (27) can be easily computed with

$$\begin{aligned} \hat{a}_i(s) &= \begin{pmatrix} T_{qa}(s) & T_{va}(s) \end{pmatrix} \begin{pmatrix} q_i(s) \\ v_i(s) \end{pmatrix} \\ &= \left(\frac{T_{qa}}{s^2} + \frac{T_{va}}{s} \right) a_i(s) := T_{aa}(s) a_i(s) \end{aligned} \tag{28}$$

[1]Technically, dCACC is not cooperative, in the sense that information exchange through wireless communication is no longer employed. However, to clearly indicate its purpose, the proposed degradation mechanism is put forward as degraded CACC rather than enhanced ACC.

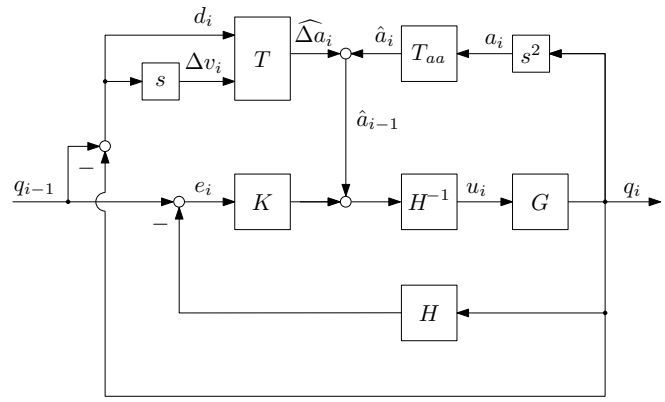

Fig. 4. Block scheme of the fallback dCACC system.

which thus only requires the locally measured acceleration a_i to be available. The transfer function $T_{aa}(s)$, involving the estimator dynamics, acts as a filter for the measured acceleration a_i, yielding the "estimated" acceleration $\hat{a}_i$, effectively synchronizing the local vehicle acceleration measurement with the estimated relative acceleration. The block diagram of the closed-loop dCACC system, as a result of this approach, is shown in Fig. 4.

IV. String stability of degraded CACC

To analyze the string stability properties of the dCACC strategy, the output of interest is chosen to be the acceleration, since this directly guarantees the existence of $\|P_1(s)\|_{\mathcal{H}_\infty}$ being the first requirement in Condition 1 for strict $\mathcal{L}_2$ string stability, as mentioned in Section II-B. The SSCS $\Gamma_{dCACC}(s)$, as defined in (6), can then be computed with $y_j(s) = a_j(s)$, $j = i, i-1$. As a result, with the closed-loop configuration given in Fig. 4, the SSCS reads

$$\Gamma_{dCACC}(s) = \frac{1}{H(s)} \frac{G(s)\big(K(s) + s^2 T_{aa}(s)\big)}{1 + G(s)K(s)}. \tag{29}$$

Note that, according to Remark 1, strict $\mathcal{L}_2$ string stability is equivalent to $\mathcal{L}_2$ string stability for the current system; moreover, since only (strict) $\mathcal{L}_2$ string stability is considered, this notion will be simply referred to as string stability.

The platoon of vehicles is string stable if also the second requirement as mentioned under Condition 1 holds, i.e., $\|\Gamma_{dCACC}(s)\|_{\mathcal{H}_\infty} \leq 1$. Furthermore, if the system is string unstable, $\|\Gamma_{dCACC}(s)\|_{\mathcal{H}_\infty}$ will exceed 1; still, in that case we would aim at making this norm as low as possible to minimize disturbance amplification. The frequency response magnitudes of $\Gamma_{CACC}(j\omega)$ from (14), $\Gamma_{dCACC}(j\omega)$ from (29), and $\Gamma_{ACC}(j\omega)$ from (15) are shown in Fig. 5(a) and 5(b) for $h = 0.3\,\mathrm{s}$ and $h = 1.3\,\mathrm{s}$, respectively. Here, the model parameters, summarized in Table I, are set according to the parameters of the test vehicles used for experiments; see Section V. From the frequency response magnitudes, it follows that for $h = 0.3\,\mathrm{s}$, only CACC appears to result in string-stable behavior, whereas for $h = 1.3\,\mathrm{s}$, both CACC and dCACC yield string stability. As expected, ACC is not string stable in either case.

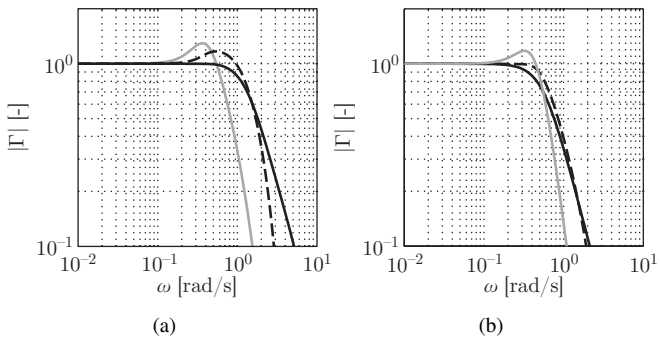

Fig. 5. SSCS frequency response magnitude for (black) CACC, (dashed) dCACC, and (grey) ACC with (a) $h = 0.3$ s and (b) $h = 1.3$ s.

TABLE I

VEHICLE AND CONTROLLER PARAMETERS.

Symbol	Value	Description
θ	0.02 s	Communication delay
τ	0.1 s	Vehicle time constant
ϕ	0.2 s	Vehicle internal time delay
k_p	0.2	Controller gain (proportional)
k_d	0.7	Controller gain (differential)
k_{dd}	0	Controller gain
a_{max}	3 m/s^2	Maximum acceleration
P_{max}	0.01	Probability of maximum acceleration
P_0	0.1	Probability of zero acceleration
α	1.25 s^{-1}	Reciprocal maneuver time constant ($1/\tau_m$)

In addition to the frequency responses, Fig. 6 shows the time responses, where the lead vehicle in a platoon of 10 vehicles follows a smooth down-step velocity profile, with $h = 0.6$ s. As a result of this disturbance, the string-stable CACC system damps the shockwave completely, whereas the dCACC and ACC systems start to propagate a shockwave. However, dCACC clearly outperforms ACC in terms of damping. For the given model and controller parameters, the string-stable time headway region for dCACC appears to be $h \geq 1.24$ s, whereas for CACC and ACC this appears to be $h \geq 0.25$ s and $h \geq 3.16$ s, respectively. Consequently, dCACC represents a significant improvement over ACC when it comes to string stability characteristics.

V. EXPERIMENTAL VALIDATION

The CACC system, with added graceful degradation feature, is implemented in two identical passenger cars (Toyota Prius III Executive), equipped with a wireless communication device that follows the ITS G5 standard [14], enabling the vehicles to communicate control-related information, e.g., the desired acceleration. The relative position of the preceding vehicle and its relative velocity are measured by a long-range radar, which is an original vehicle component in this case. Furthermore, a real-time platform executes the CACC with a sampling time of $t_s = 0.01$ s, yielding the desired vehicle acceleration which is then forwarded to a low-level acceleration controller of the vehicle.

The lead vehicle is velocity controlled, with a reference velocity $v_r(t)$ that is generated based on the requirement to

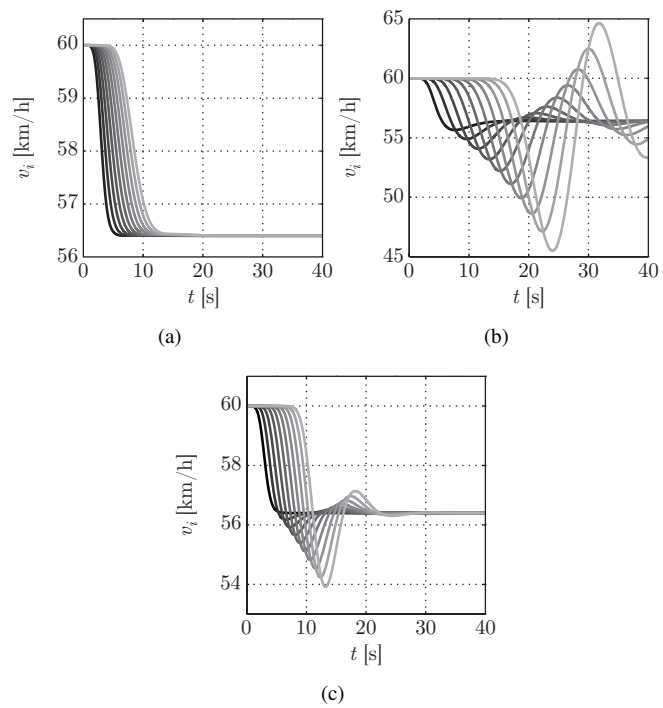

Fig. 6. Time response of the velocity $v_i(t)$, $i = 1, \ldots, 10$ (black–light grey), subject to (a) CACC, (b) ACC, and (c) dCACC.

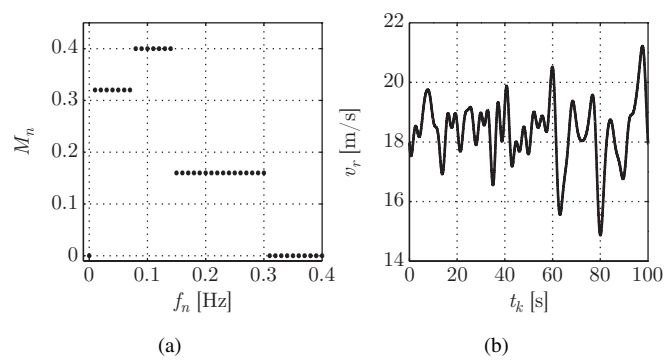

Fig. 7. Velocity test signal used for identification of the controlled vehicle platoon; (a) frequency-domain magnitude and (b) time-domain signal.

provide sufficient frequency content for performing a non-parametric system identification, in particular to identify the SSCS function in the relevant frequency range. Towards this end, the selected signal is a random-phase multisine signal that covers the frequency range $f \in [0, 0.3]$ Hz. This range of excitation, as well as the frequency weighting factors M_n, with $n = 0, 1, \ldots, \frac{N}{2} - 1$ and N being the number of frequency intervals up to the sampling frequency $f_s = 1/t_s$, are chosen based on the frequency content needed for SSCS identification. The chosen frequency-domain magnitudes M_n of the test signal, as a function of the discrete frequency $f_n = n\Delta f$, with frequency interval $\Delta f = f_s/N$, are shown in Fig. 7(a); the resulting discrete-time signal $v_r(k)$ at time $t_k = kt_s$ with $k = 0, 1, \ldots, N-1$, is shown in Fig. 7(b).

In order to run the dCACC system in the test vehicles, the relative-acceleration estimator in (27) has been implemented

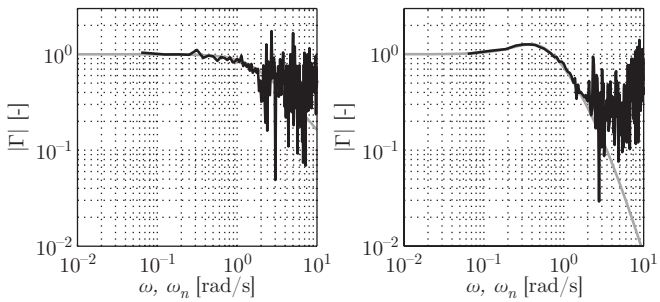

(a) (b)

Fig. 8. SSCS frequency response magnitude: (black) experimental and (grey) theoretical, of the system subject to (a) CACC and (b) ACC.

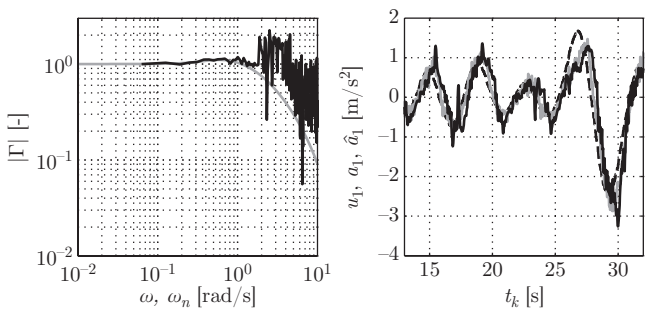

(a) (b)

Fig. 9. dCACC characteristics: (a) SSCS frequency response magnitude: (black) experimental and (grey) theoretical, and (b) lead vehicle acceleration: (dashed black) desired, (solid grey) measured, and (solid black) estimated.

in the follower vehicle using the discrete-time equivalent of the filter equation (23), with measurement input vector $y^{\mathrm{T}}(k) = \big(d_2(k)\ \Delta v_2(k)\big)$ being the radar output, and with the state vector $\hat{x}^{\mathrm{T}}(k) = \big(\hat{d}_2(k)\ \widehat{\Delta v}_2(k)\ \widehat{\Delta a}_2(k)\big)$. This yields the estimated relative acceleration $\widehat{\Delta a}_2(k)$, based on which the absolute target vehicle acceleration $a_1(k)$ is estimated by adding the filtered locally measured acceleration $\hat{a}_2(k)$, using the discrete-frequency equivalent of $T_{aa}(s)$ in (28) combined with an onboard acceleration sensor.

Using the measured test data, a nonparametric system identification is performed to compute $|\Gamma_{CACC}(j\omega_n)|$, $|\Gamma_{ACC}(j\omega_n)|$, and $|\Gamma_{dCACC}(j\omega_n)|$, with $\omega_n = n2\pi\Delta f$. Subsequently, these are compared with the theoretical values, i.e., through equations (14), (15), and (29), respectively, using $h = 0.6\,\mathrm{s}$ headway time. The results are shown in Fig. 8(a), 8(b), and 9(a). It can be clearly seen that the experimental results match well with the theoretical ones in the frequency range of excitation. It can thus be concluded that the experiments confirm the improvement with respect to string stability obtained with dCACC compared to the conventional fallback scenario. Consequently, smaller time headways are feasible under severe packet loss.

Finally, Fig. 9(b) shows the desired acceleration $u_1(k)$ and the actual measured acceleration $a_1(k)$ of the lead vehicle, both received in the follower vehicle via the communication link, as well as the estimated acceleration $\hat{a}_1(k)$, computed locally in the follower vehicle. As can be seen in this figure, $\hat{a}_1(k)$ provides a satisfactory estimation of $a_1(k)$, but shows a noticeable phase lag with respect to $u_1(k)$, which accounts for the degraded string stability performance of dCACC.

VI. Conclusion

A graceful degradation technique for CACC was presented, serving as an alternative fallback scenario to ACC. The idea behind the proposed approach is to obtain the minimum loss of functionality of CACC when the wireless communication link fails. The proposed strategy uses an estimation of the preceding vehicle's current acceleration as a replacement to the desired acceleration which would normally be communicated. It was shown that the performance, in terms of string stability of degraded CACC (dCACC), can be maintained at a much higher level compared to an ACC fallback scenario. Both theoretical as well as experimental results showed that the dCACC system outperforms the ACC fallback scenario with respect to string stability characteristics by reducing the minimum string-stable time headway to less than half of the required value in case of ACC.

References

[1] R. Rajamani and C. Zhu, "Semi-autonomous adaptive cruise control systems," *IEEE Trans. Veh. Technol.*, vol. 51, no. 5, pp. 1186–1192, Sep. 2002.

[2] S. E. Shladover, D. Su, and X.-Y. Lu, "Impacts of cooperative adaptive cruise control on freeway traffic flow," in *Proc. 91st TRB Annual Meeting*, Washington, D.C., Jan. 22–26 2012, pp. 1–17.

[3] R. Ramakers, K. Henning, S. Gies, D. Abel, and H. Max, "Electronically coupled truck platoons on german highways," in *Proc. IEEE Int. Conf. Syst., Man, Cybernetics*, Oct. 11–14 2009, pp. 2409–2414.

[4] D. Eckhoff, N. Sofray, and R. German, "A performance study of cooperative awareness in ETSI ITS G5 and IEEE WAVE," in *Proc. 10th Annual Conf. Wireless On-Demand Network Syst. Services*, Banff, Alberta, Canada, Mar. 18–20 2013, pp. 196–200.

[5] S. Öncü, N. Wouw, W. P. M. H. Heemels, and H. Nijmeijer, "String stability of interconnected vehicles under communication constraints," in *Proc. IEEE 51st Annual Conf. Decision Contr.*, Maui, HI, USA, Dec. 10–13 2012, pp. 2459–2464.

[6] J. Ploeg, N. Wouw, and H. Nijmeijer, "$\mathcal{L}_p$ string stability of cascaded systems: Application to vehicle platooning," *IEEE Trans. Control Syst. Technol.*, 2013, accepted.

[7] J. Ploeg, B. T. M. Scheepers, E. Nunen, N. Wouw, and H. Nijmeijer, "Design and experimental evaluation of cooperative adaptive cruise control," in *Proc. 14th Int. IEEE Conf. Intell. Transp. Syst.*, Washington D.C., USA, Oct. 5–7 2011, pp. 260–265.

[8] D. Swaroop and J. K. Hedrick, "String stability of interconnected systems," *IEEE Trans. Autom. Control*, vol. 41, no. 3, pp. 349–357, Mar. 1996.

[9] R. F. Curtain, O. V. Iftime, and H. J. Zwart, "System theoretic properties of a class of spatially invariant systems," *Automatica*, vol. 45, no. 7, pp. 1619–1627, Jul. 2009.

[10] R. A. Singer, "Estimating optimal tracking filter performance for manned maneuvering targets," *IEEE Trans. Aerosp. Electron. Syst.*, vol. AES-6, no. 4, pp. 473–483, Jul. 1970.

[11] G. Lijster, "A radar-based enhanced control algorithm for adaptive cruise control," Master's thesis DC.2012.016, Eindhoven Univ. Technol., Dept. Mech. Eng., Apr. 2012.

[12] X. R. Li and V. P. Jilkov, "A survey of maneuvering target tracking–part IV: Decision-based methods," in *Proc. SPIE Conf. Signal. Data Process. Small Targets*, Apr. 2002, pp. 4728–4760.

[13] P. S. Maybeck, *Stochastic Models, Estimation, and Control*, ser. Mathematics in Science and Engineering. Academic Press, Inc, 1979, vol. 141.

[14] E. G. Ström, "On medium access and physical layer standards for cooperative intelligent transport systems in Europe," *Proc. IEEE*, vol. 99, no. 7, pp. 1183–1188, 2011.